

# Optimal-observable analysis of possible new physics in $B \rightarrow D^{(*)}\tau\nu_\tau$

Srimoy Bhattacharya, Soumitra Nandi, and Sunando Kumar Patra  
*Indian Institute of Technology, North Guwahati, Guwahati 781039, Assam, India*

We study all possible observables in  $B \rightarrow D^{(*)}\tau\nu_\tau$  with new physics (NP), including new vector, scalar and tensor interactions, and investigate the prospects of extracting NP Wilson coefficients with optimal observables. Analysis of the full  $q^2$  integrated branching fractions of  $B \rightarrow D^{(*)}\tau\nu_\tau$  show that the overall sensitivity of the observables of  $B \rightarrow D\tau\nu_\tau$  is more towards the scalar current, whereas the bin-by-bin analysis of  $q^2$  distribution of the differential branching fraction points to regions of  $q^2$  sensitive to tensor interactions. Interestingly, the observables in  $B \rightarrow D^*\tau\nu_\tau$  are more sensitive to tensor interactions, and bin-by-bin analysis of this mode shows the distinct regions of  $q^2$  sensitive to vector or scalar interactions. In addition to that, the  $\tau$  polarisation asymmetry is found to be more sensitive to NP compared to the other observables, in both decay modes.

PACS numbers:

## I. INTRODUCTION

Measurements of branching fractions and other related observables in semileptonic decays of  $B$  meson to  $\tau$  can be interesting for an indirect probe of NP. Earlier measurements on  $R(D^{(*)}) = \mathcal{BR}(B \rightarrow D^{(*)}\tau\nu_\tau)/\mathcal{BR}(B \rightarrow D^{(*)}\ell\nu_\ell)$  by Belle [1] and BABAR collaborations [2] have shown some deviations from their Standard Model (SM) predictions [3], indicating a possible signature of NP in  $b \rightarrow c\tau\nu_\tau$  transitions. Several authors have tried to explain the observation in various NP scenarios [4–6], as well as in a model-independent way [7–9]. In order to distinguish between the possible signatures of NP, the study of NP in  $q^2$  distribution of differential branching fractions in  $B \rightarrow D^{(*)}\tau\nu_\tau$ , various correlations among  $\tau$  forward-backward asymmetry and  $\tau$  polarization asymmetry has been examined in the Ref. [5, 10, 11]. Recently, a  $2.1\sigma$  deviation in the measurement of  $R(D^*)$  has been reported by LHCb collaboration [12]; Belle collaboration has also announced their most recent results on  $R(D^{(*)})$  and measured values are consistent with the SM within error bars [13].

So far, the constraints on the new couplings are obtained assuming their presence one at a time [5, 8]. If we consider all the interactions together, then it will be an impossible task to extract all the couplings from a single measurement. However, if one can reduce the number of coupling parameters by imposing certain constraints on the full set of parameters, only then it is possible to obtain meaningful errors on the couplings, although the information lost due to various assumptions cannot be retrieved. Therefore, it will be useful to have independent couplings, parametrised in such a way that the measured errors on different parameters are uncorrelated. On the other hand, it is not necessary for a particular observable to have equal sensitivity to different types of NP operators. Therefore, it is useful to know how an observable can be optimised to guarantee the maximal sensitivity to a particular type of NP interaction, which in turn will help us select observables suitable for the extraction of a particular type of coupling. Hence, from a phenomenological point of view, it is important to find out the significance of different types of NP interaction, to an observable. To achieve this goal, we use the optimal-observable analysis using the invariant mass squared  $q^2$ , of the lepton-neutrino system. We construct the optimal observable to identify the NP structure that can be best extracted from a particular observable, with reasonable statistics. It also provides a deeper understanding of the sensitivity that can be best obtained by any method, for a certain process. This technique has been widely used in collider phenomenology [14–19].

In this article, we analyse the  $q^2$  distribution of the differential branching fractions,  $R(D^{(*)})$ , the  $\tau$  polarisation asymmetries, forward backward asymmetries of the decay  $B \rightarrow D^{(*)}\tau\nu_\tau$ , and  $D^*$  polarisation asymmetry. We include all possible non-standard four-fermi effective interactions of the lowest dimension, and estimate the expected statistical uncertainties in the extraction of various NP Wilson coefficients that can contribute to  $B \rightarrow D^{(*)}\tau\nu_\tau$ .

## II. METHODOLOGY

The most general effective Hamiltonian describing the  $b \rightarrow c\tau\nu_\tau$  transitions with all possible four-fermi operators in the lowest dimension is given by [8]

$$\begin{aligned} \mathcal{H}_{eff} = & \frac{4G_F}{\sqrt{2}} V_{cb} \left[ (1 + C_{V_1}) \mathcal{O}_{V_1} + C_{V_2} \mathcal{O}_{V_2} \right. \\ & \left. + C_{S_1} \mathcal{O}_{S_1} + C_{S_2} \mathcal{O}_{S_2} + C_T \mathcal{O}_T \right], \end{aligned} \quad (1)$$

where the operator basis is defined as

$$\begin{aligned} \mathcal{O}_{V_1} &= (\bar{c}_L \gamma^\mu b_L)(\bar{\tau}_L \gamma_\mu \nu_{\tau L}), \quad \mathcal{O}_{V_2} = (\bar{c}_R \gamma^\mu b_R)(\bar{\tau}_L \gamma_\mu \nu_{\tau L}), \\ \mathcal{O}_{S_1} &= (\bar{c}_L b_R)(\bar{\tau}_R \nu_{\tau L}), \quad \mathcal{O}_{S_2} = (\bar{c}_R b_L)(\bar{\tau}_R \nu_{\tau L}), \\ \mathcal{O}_T &= (\bar{c}_R \sigma^{\mu\nu} b_L)(\bar{\tau}_R \sigma_{\mu\nu} \nu_{\tau L}), \end{aligned} \quad (2)$$

and the corresponding Wilson coefficients are given by  $C_W (W = V_1, V_2, S_1, S_2, T)$ . In this basis, neutrinos are assumed to be left handed. Our main focus is on the  $q^2$  distribution of differential decay rate  $d\Gamma/dq^2$  in  $B \rightarrow D^{(*)}\tau\nu_\tau$ . The complete expressions are given in ref.[5].

As mentioned earlier, the optimal-observable analysis is a technique to systematically estimate the statistical uncertainties of the measurable parameters while extracting them from some observable. Elaborate discussions on this technique can be found in references [15–18]. In order to apply this technique to  $B \rightarrow D^{(*)}\tau\nu_\tau$ , it is necessary to express the  $q^2$  distribution of the differential decay rate as

$$\frac{d\Gamma(B \rightarrow D^{(*)}\tau\nu_\tau)}{dq^2} = \sum_i C_i f_i(q^2), \quad (3)$$

where  $C_i$ s are functions of  $C_W$ s. The theoretical expressions for  $C_i$ s, along with the  $f_i(q^2)$ s, can be extracted from a direct comparison between the similar terms on both sides of eq.(3). The coefficients  $C_i$ , relevant for the branching fractions in  $B \rightarrow D^{(*)}\tau\nu_\tau$ , are given in Table I, and the corresponding  $f_i(q^2)$ s are given in the Appendix (Table XIV).

$C_i$ \diagdown Obs	$d\mathcal{B}/dq^2$ in $B \rightarrow D\tau\nu_\tau$	$d\mathcal{B}/dq^2$ in $B \rightarrow D^*\tau\nu_\tau$
$C_1$	$ 1 + C_{V_1} + C_{V_2} ^2$	$ 1 + C_{V_1} ^2 +  C_{V_2} ^2$
$C_2$	$ C_{S_1} + C_{S_2} ^2$	$\text{Re}[(1 + C_{V_1})C_{V_2}^*]$
$C_3$	$ C_T ^2$	$ C_{S_1} - C_{S_2} ^2$
$C_4$	$\text{Re}[(1 + C_{V_1} + C_{V_2})(C_{S_1}^* + C_{S_2}^*)]$	$ C_T ^2$
$C_5$	$\text{Re}[(1 + C_{V_1} + C_{V_2})C_T^*]$	$\text{Re}[(1 + C_{V_1} - C_{V_2})(C_{S_1}^* - C_{S_2}^*)]$
$C_6$	–	$\text{Re}[(1 + C_{V_1})C_T^*]$
$C_7$	–	$\text{Re}[C_{V_2}C_T^*]$

TABLE I:  $C_i$ s as defined in eq.(3). The observable  $P_\tau^R(q^2)$  contains the same set of  $C_i$ s.

The goal of this technique is to extract  $C_i$ s, which can be done by defining suitable weighting functions  $w_i(q^2)$  such as  $C_i = \int w_i(q^2)(d\Gamma/dq^2)dq^2$ . In general various choices of  $w_i$ s are possible. However, there is a unique choice for which the resulting error in the extraction of  $C_i$  is minimized<sup>1</sup>, and these functions are given by

$$w_i(q^2) = \sum_j \frac{X_{ij} f_j(q^2)}{d\Gamma/dq^2}, \quad (4)$$

where  $X_{ij}$  is the inverse of  $M_{ij}$  which is defined as

$$M_{ij} = \int dq^2 \frac{f_i(q^2) f_j(q^2)}{f_{SM}(q^2)}. \quad (5)$$

<sup>1</sup>  $C_i$ s are minimised in a sense that the whole covariance matrix is at a stationary point in terms of varying the functional forms of  $w_i(q^2)$  while maintaining  $\int w_i(q^2) f_k(q^2) = \delta_{ik}$ .

In the above expression,  $f_{SM}(q^2)$  can be obtained from eq.(3) by setting  $C_W = 0$ , while  $C_{SM} = 1$ . Hence, using eqs. (4), and (5) the statistical uncertainties in  $C_i$  extracted from the branching fractions can be obtained as [16, 17]

$$|\delta C_i| = \sqrt{\frac{X_{ii} \mathcal{B}(B \rightarrow D^{(*)} \tau \nu_\tau)^{exp}}{N_{sig}}} = \sqrt{\frac{X_{ii}}{\sigma_P \mathcal{L}_{eff}}}, \quad (6)$$

where  $\mathcal{B}^{exp} = (1/\Gamma) \int dq^2 d\Gamma/dq^2$  is the total branching fraction in the decay  $B \rightarrow D^{(*)} \tau \nu_\tau$  with  $\Gamma$  as the total decay width.  $N_{sig}$  is the total number of events. As given in eq.(6), the errors are also related to the production cross section  $\sigma_P (= \sigma_{B \rightarrow D^{(*)} \tau \nu_\tau} / \mathcal{B}(B \rightarrow D^{(*)} \tau \nu_\tau))$ , and the effective luminosity  $\mathcal{L}_{eff} = \mathcal{L}_{int} \epsilon_s$ , where  $\mathcal{L}_{int}$  and  $\epsilon_s$  are the integrated luminosity and reconstruction efficiency respectively<sup>2</sup>. The above-mentioned method, and the equations like (5) and (6), can be generalised for any other observables in  $B \rightarrow D^{(*)} \tau \nu_\tau$  decay.

Since the data is consistent with the SM, if there is NP in  $B \rightarrow D^{(*)} \tau \nu_\tau$  decays, the effect is expected to be small compared to their SM counterpart. The earlier model independent analysis [8], which is based on data by BABAR [2], shows that zero value of the new Wilson coefficients are consistent with the data. Therefore, we choose our starting point as  $C_W = 0$  and find out errors in the extraction of those coefficients around that point. In addition to that, we assume that the error on  $C_i$  could be captured sufficiently well by just the leading-order terms.

We focus on the following observables:

- The branching fractions, obtained by integrating the differential branching fractions over the full  $q^2$  region, normalised by the full  $q^2$  integrated branching fraction  $\mathcal{B}_\ell = \mathcal{B}(B \rightarrow D^{(*)} \ell \nu_\ell)$ .

$$R(D^{(*)}) = \int dq^2 R_{D^{(*)}}(q^2), \quad (7)$$

with

$$R_{D^{(*)}}(q^2) = \frac{1}{\mathcal{B}_\ell} \frac{d\mathcal{B}(B \rightarrow D^{(*)} \tau \nu_\tau)}{dq^2}. \quad (8)$$

- $\tau$  polarisation asymmetry which we defined as  $P_\tau^{R^{(*)}}(q^2) = P_\tau(q^2) R_{D^{(*)}}(q^2)$ , where

$$P_\tau(q^2) = \frac{d\Gamma_{\lambda=1/2}/dq^2 - d\Gamma_{\lambda=-1/2}/dq^2}{d\Gamma_{\lambda=1/2}/dq^2 + d\Gamma_{\lambda=-1/2}/dq^2}. \quad (9)$$

- $\tau$  forward-backward asymmetry  $\mathcal{A}_{FB}^{R^{(*)}}(q^2) = \mathcal{A}_{FB}(q^2) R_{D^{(*)}}(q^2)$ , where

$$\begin{aligned} \mathcal{A}_{FB}(q^2) &= \frac{\int_0^1 \frac{d\Gamma}{dq^2 d\cos\theta} d\cos\theta - \int_{-1}^0 \frac{d\Gamma}{dq^2 d\cos\theta} d\cos\theta}{\int_{-1}^1 \frac{d\Gamma}{dq^2 d\cos\theta} d\cos\theta} \\ &= \frac{b_\theta(q^2)}{d\Gamma/dq^2}, \end{aligned} \quad (10)$$

where  $\theta$  is the angle that  $\tau$  makes with the  $\bar{B}$  in the rest frame of  $\tau \bar{\nu}$ . The expressions for  $b_\theta(q^2)$  are given in [5].

- $D^*$  longitudinal polarisation asymmetry  $P_{D^*}^R(q^2) = P_{D^*}(q^2) R_{D^*}(q^2)$ , where

$$P_{D^*}(q^2) = \frac{\frac{d\Gamma}{dq^2}(\lambda_{D^*=0})}{\frac{d\Gamma}{dq^2}(\lambda_{D^*=0}) + \frac{d\Gamma}{dq^2}(\lambda_{D^*=1}) + \frac{d\Gamma}{dq^2}(\lambda_{D^*=-1})}. \quad (11)$$

<sup>2</sup> As we know that the cross section  $\sigma_{a \rightarrow b} = \sigma_a \Gamma_b / \Gamma$ , therefore, we can define  $\sigma_{B \rightarrow D^{(*)} \tau \nu_\tau} = \sigma_P \mathcal{B}(B \rightarrow D^{(*)} \tau \nu_\tau)$ , where  $\sigma_P$  is the  $B\bar{B}$  production cross section. If we redefine our observable as  $\sigma_{B \rightarrow D^{(*)} \tau \nu_\tau}$  than the errors in  $C_i$  can be written as

$$\begin{aligned} \delta C_i &= \sqrt{\frac{X'_{ii} \sigma_{B \rightarrow D^{(*)} \tau \nu_\tau}}{N_{sig}}} = \sqrt{\frac{X'_{ii}}{\mathcal{L}_{eff}}} = \sqrt{\frac{X_{ii}}{\sigma_P \mathcal{L}_{eff}}} \\ &= \sqrt{\frac{X_{ii} \mathcal{B}(B \rightarrow D^{(*)} \tau \nu_\tau)^{exp}}{N_{sig}}}, \end{aligned}$$

since  $X'_{ii} = X_{ii} / \sigma_P$ .

$C_i \backslash$ Obs	$\mathcal{A}_{FB}^R(q^2)$	$\mathcal{A}_{FB}^{R*}(q^2)$	$P_{D^*}(q^2)$
$C_1$	$ 1 + C_{V_1} + C_{V_2} ^2$	$ 1 + C_{V_1} ^2 -  C_{V_2} ^2$	$ 1 + C_{V_1} - C_{V_2} ^2$
$C_2$	$Re[(1 + C_{V_1} + C_{V_2})(C_{S_1}^* + C_{S_2}^*)]$	$ 1 + C_{V_1} - C_{V_2} ^2$	$ C_{S_1} - C_{S_2} ^2$
$C_3$	$Re[(1 + C_{V_1} + C_{V_2})C_T^*]$	$ C_T ^2$	$ C_T ^2$
$C_4$	$Re[(C_{S_1} + C_{S_2})C_T^*]$	$Re[(1 + C_{V_1} - C_{V_2})(C_{S_1}^* - C_{S_2}^*)]$	$Re[(1 + C_{V_1} - C_{V_2})(C_{S_1}^* - C_{S_2}^*)]$
$C_5$	–	$Re[(1 + C_{V_1})C_T^*]$	$Re[(1 + C_{V_1} - C_{V_2})C_T^*]$
$C_6$	–	$Re[C_{V_2}C_T^*]$	–
$C_7$	–	$Re[(C_{S_1} - C_{S_2})C_T^*]$	–

TABLE II: Expressions of  $C_i$ s for different observables.

In the above definitions, the detailed expression for  $d\Gamma/dq^2$  are taken from ref.[5]. For forward backward asymmetries and the  $D^*$  polarisation, the  $C_i$ s and the corresponding  $f_i(q^2)$ s are given in the Tables II, and in the Appendix XVI.

All the above-mentioned observables are expected to be measured with good statistics in future experiments like Belle-II and LHCb. The corresponding errors on  $C_i$  can be obtained using the following relation

$$|\delta C_i| = \sqrt{\frac{X_{ii}^\ell}{\mathcal{B}_\ell \sigma_P \mathcal{L}_{eff}}}, \quad (12)$$

where  $X_{ii}^\ell = X_{ii}\mathcal{B}_\ell$ .

### III. ANALYSIS

There are varieties of NP models that can contribute to  $B \rightarrow D^{(*)}\tau\nu_\tau$ , and the characteristics of those models could be very different. For example, two higgs doublet model (2HDM) has only scalar-type interactions, new gauge boson  $Z'$  and  $W'$  take part only in vector-type interactions, the model with leptoquarks has both the scalar or vector-type interactions [20]<sup>3</sup>, the extra dimensional models have tensor interaction in addition to scalar or vector-type interactions [21].

In our analysis of the decay  $B \rightarrow D\tau\nu_\tau$ , it will be hard to estimate the uncertainties in the extractions of  $C_{V_1}$  and  $C_{V_2}$ , because they cannot be singled out from their SM counterpart (same  $f_i$ s). The similar argument holds for the decay  $B \rightarrow D^*\tau\nu_\tau$ , however, in this decay we can estimate the error in the extraction of  $Re(C_{V_2})$ , see for instance Tables I and XV where  $f_2$  associated with  $C_2$  is different from  $f_1$  associated with  $C_1$ . In Table III, we list a few interesting cases of NP relevant for the observables in  $B \rightarrow D\tau\nu_\tau$ . In many cases, we assume  $C_V = C_{V_1} + C_{V_2} = 0$ , however, the assumption  $C_V \neq 0$  will lead to the same set of parameters that has to be simultaneously extracted, if it is assumed that  $C_V \ll 1$ . Under such conditions  $C_1$  can be treated as the Wilson coefficient of the vector operator. The different NP cases related to the observables in  $B \rightarrow D^*\tau\nu_\tau$  are given in Tables IV, V and VI respectively. In most cases, we assume  $C_{V_1} = 0$ , though the same set of parameters can be obtained without this assumption if  $C_{V_1} \ll 1$ . For  $\tau$  forward-backward asymmetry in  $B \rightarrow D^*\tau\nu_\tau$ , we discuss mostly the cases with  $C_{V_2} = 0$ . In such cases,  $C_1 = C_2$ , and therefore we need to merge  $f_1(q^2)$  and  $f_2(q^2)$  into  $f(q^2)(= f_1(q^2) + f_2(q^2))$  for the analysis. In all the other cases, when  $C_{V_2} \neq 0$ , the extracted uncertainties are large. We will discuss only one such interesting case.

Cases	Assumptions
$a$	$C_i \neq 0, i = 1, ..5$
$b$	$Re(C_T) = 0$
$c$	$Re(C_S) = 0$
$d$	$Re(C_S) = 0$ and $Re(C_T) = 0$
$e$	$C_T = 0$
$f$	$C_S = 0$

TABLE III: Cases relevant for  $R_D(q^2)$ ,  $P_\tau^R(q^2)$  and  $\mathcal{A}_{FB}^R(q^2)$ . Here  $C_S = C_{S_1} + C_{S_2}$ , and in all the cases  $C_{V_1} + C_{V_2} = 0$ .

The numerical values of all the relevant parameters, like the form-factors, various masses and lifetimes are taken from ref. [22], and for the analysis we choose the central values of all the form-factors. The errors of the form-factors

<sup>3</sup> Although the model with scalar-type interactions may also contribute to tensor Wilson coefficients by Fierz reordering.

Cases	Assumptions
$a^*$	$C_S = 0$
$b^*$	$C_{V_2} = 0$
$c^*$	$C_T = 0$
$d^*$	$Re(C_S) = 0, C_{V_2} = 0$
$e^*$	$Re(C_S) = 0, C_T = 0, Im(C_{V_2}) = 0$
$f^*$	$C_S = 0, Re(C_T) = 0, Im(C_{V_2}) = 0$
$g^*$	$C_{V_2} = 0, Re(C_T) = 0, Re(C_S) = 0$
$h^*$	$C_{V_2} = 0, C_T = 0$
$i^*$	$C_{V_2} = 0, C_S = 0$
$j^*$	$Re(C_S) = 0, Re(C_T) = 0, Im(C_{V_2}) = 0$
$k^*$	$C_S = 0, C_T = 0$

TABLE IV: Different cases related to  $R_{D^*}(q^2)$  and  $P_\tau^{R^*}(q^2)$  in  $B \rightarrow D^* \tau \nu_\tau$ . Here  $C_S = C_{S_1} - C_{S_2}$ , and in all the cases  $C_{V_1} = 0$ .

Cases	Assumptions
1*	$C_S = 0$
2*	$C_{V_2} = 0, Re(C_T) = 0$
3*	$C_{V_2} = 0, Re(C_S) = 0$
4*	$C_{V_2} = 0, Re(C_T) = 0, Im(C_S) = 0$
5*	$C_{V_2} = 0, C_S = 0$
6*	$C_{V_2} = 0, Re(C_S) = 0, Re(C_T) = 0$
7*	$C_{V_2} = 0, C_T = 0$

TABLE V: Cases relevant in  $\mathcal{A}_{FB}^{R^*}(q^2)$  with  $C_{V_1} = 0$ .

Cases	Assumptions
A	$C_i \neq 0, i = 1, \dots, 5$
B	$Re(C_T) = 0$
C	$Re(C_S) = 0$
D	$Re(C_S) = 0, Re(C_T) = 0$
E	$C_T = 0$
F	$C_S = 0$
G	$Re(C_S) = 0, C_T = 0$
H	$Re(C_T) = 0, C_S = 0$

TABLE VI: NP cases relevant in  $D^*$  polarisation asymmetry. Here,  $C_V = C_{V_1} - C_{V_2} = 0$ .

are considered while we estimate the additional errors on the extracted coefficients. We choose as benchmark values  $\mathcal{B}(B \rightarrow D \ell \nu) = 2.32\%$ ,  $\mathcal{B}(B \rightarrow D^* \ell \nu) = 5.31\%$ ,  $\sigma_P = 1105.63 \text{ pb}$ , and  $\mathcal{L}_{eff} = 1 \text{ fb}^{-1}$ .

Decay	$B \rightarrow D \tau \nu_\tau$			
Cases	$b$		$c$	
	Obs.			
$ \delta C_i $	$R(D)$	$P_\tau^R$	$R(D)$	$P_\tau^R$
$\delta C_1$	0.60	0.37	0.60	0.37
$\delta  C_S ^2$	1.03	0.04	0.13	0.08
$\delta  C_T ^2$	0.62	0.70	1.12	0.72
$\delta(Re(C_S))$	1.31	0.06	-	-
$\delta(Re(C_T))$	-	-	1.15	0.12

TABLE VII: Numerical values of the  $1\sigma$  error on  $C_i$ s extracted from  $R(D)$  and  $P_\tau^R$ . For the cases  $Re(C_i) = 0$ ,  $\delta |C_i|^2 = \delta(Im^2(C_i))$ .

In Table VII, we list our main results of the uncertainties in  $C_i$  extracted from the analysis of the  $R(D)$  and  $P_\tau^R$  corresponding to different cases listed in Table III, while those for  $R(D^*)$  and  $P_\tau^{R^*}$ , corresponding to the cases listed in Table IV, are given in Table VIII. For a given case, we estimate the statistical significance of the simultaneous extraction of  $C_i$ s. The numerical values are given only for parameters relevant to a particular case, while the rest are set to zero.

In some more simplified cases, where the number of non-zero NP parameters are less, we compute the  $\chi^2$ , which is

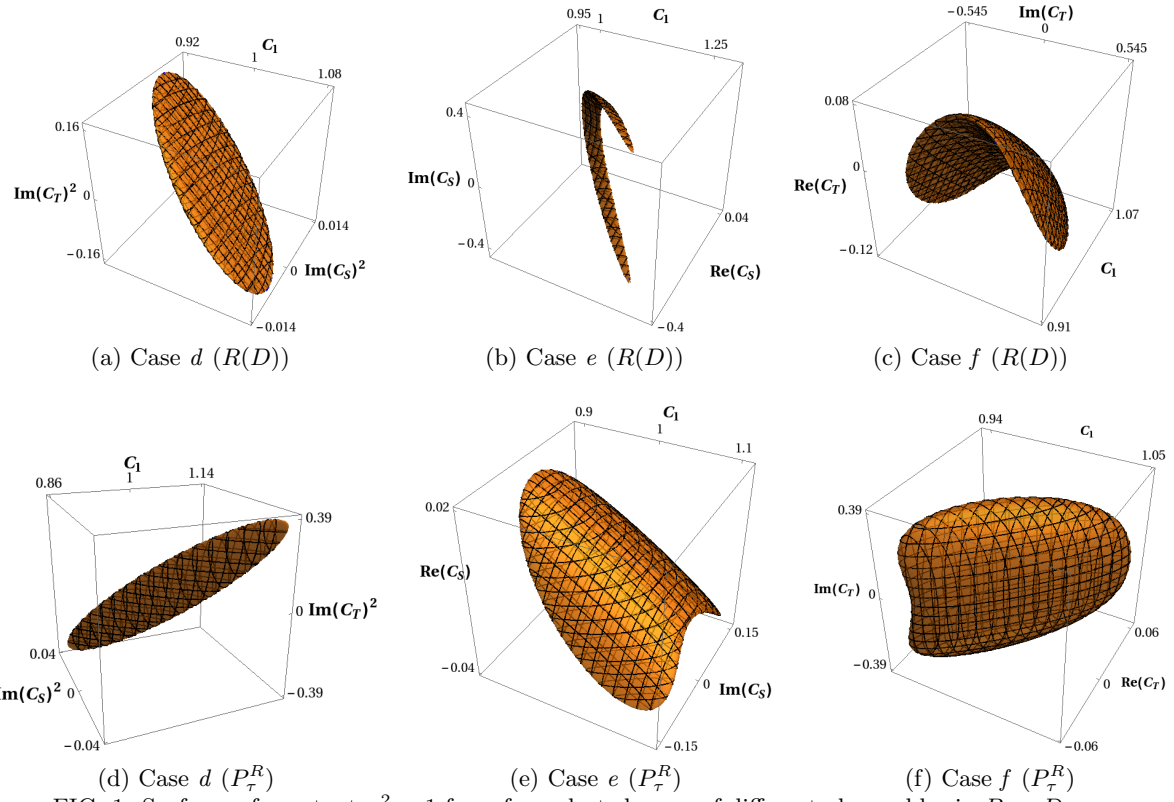


FIG. 1: Surfaces of constant  $\chi^2 = 1$  for a few selected cases of different observables in  $B \rightarrow D\tau\nu_\tau$ .

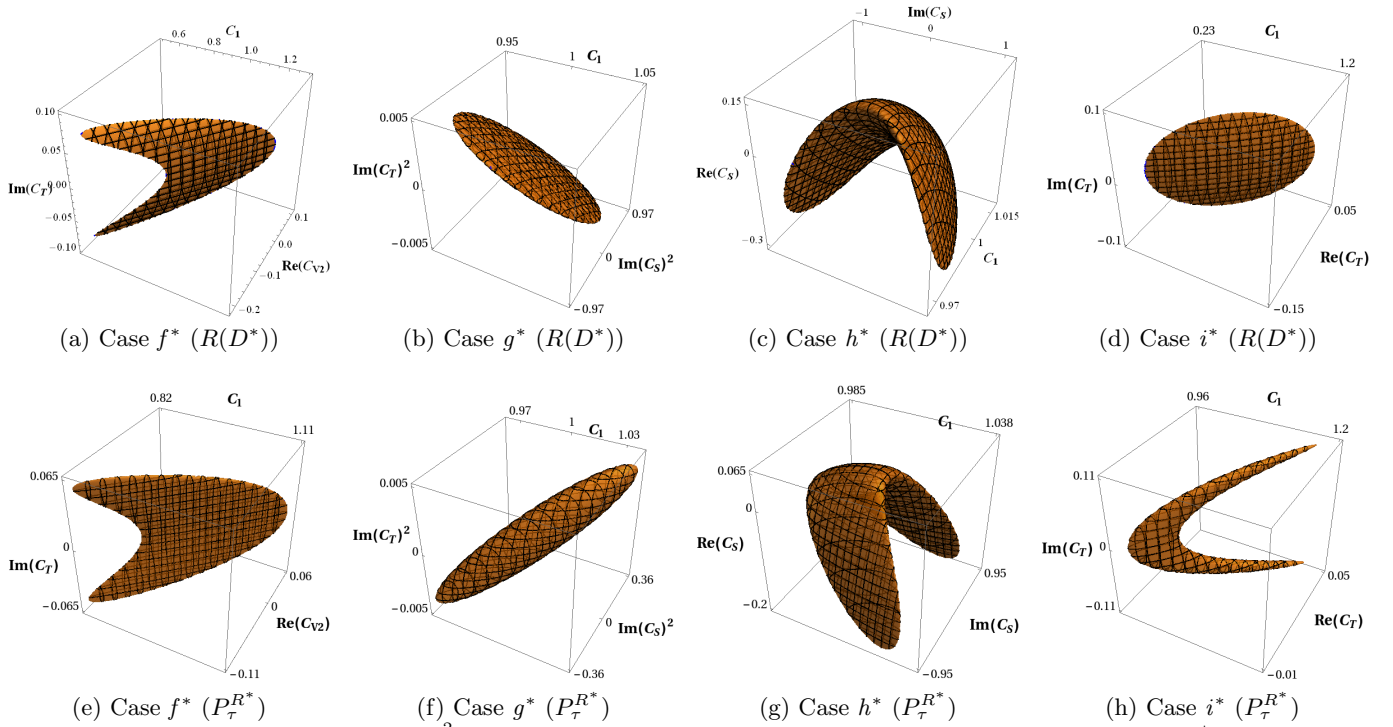


FIG. 2: Surfaces of constant  $\chi^2 = 1$  for a few selected cases of different observables shown in  $B \rightarrow D^*\tau\nu_\tau$ .

Decay Modes	$B \rightarrow D^* \tau \nu_\tau$									
	$a^*$		$b^*$		$c^*$		$d^*$		$e^*$	
Cases	$R(D^*)$	$P_\tau^{R^*}$	$R(D^*)$	$P_\tau^{R^*}$	$R(D^*)$	$P_\tau^{R^*}$	$R(D^*)$	$P_\tau^{R^*}$	$R(D^*)$	$P_\tau^{R^*}$
$\delta C_1$	7.22	13.70	289.17	116.82	28.44	14.08	2.01	0.65	1.28	1.25
$\delta  C_S ^2$	-	-	629.08	204.37	56.25	29.65	1.00	1.73	3.68	1.83
$\delta  C_T ^2$	4.30	1.96	11.86	4.62	-	-	0.03	0.04	-	-
$\delta(Re(C_S))$	-	-	529.3	191.49	6.81	2.20	-	-	-	-
$\delta(Re(C_T))$	28.27	36.92	36.71	45.37	-	-	0.35	0.24	-	-
$\delta(Re(C_{V_2}))$	47.10	18.51	-	-	14.21	7.03	-	-	0.63	0.63
$\delta Re[C_{V_2} C_T^*]$	15.70	17.19	-	-	-	-	-	-	-	-

TABLE VIII: Numerical values of the  $1\sigma$  error on  $C_{is}$  extracted from  $R(D^*)$  and  $P_\tau^{R^*}$ . For the cases  $Re(C_i) = 0$ ,  $\delta |C_i|^2 = \delta(Im^2(C_i))$ .

defined as

$$\chi^2 = \sum_{i,j} (C_i - C_i^0)(C_j - C_j^0) V_{ij}^{-1},$$

where,  $V_{ij} = \frac{X_{ij}}{\mathcal{B}_\ell \sigma_P \mathcal{L}_{eff}}$ . (13)

The  $C_i^0$ s are the seed values, which can be considered as model inputs; as discussed earlier, we choose  $C_i^0 = 0$ , for  $i \neq 1$ , and  $C_1^0 = 1$ . The  $\chi^2 = 1$  surfaces are perfect ellipsoids in  $C_i$  basis, and they indicate the  $\pm 1\sigma$  errors in the determination of  $C_i$ s. The constant  $\chi^2 = 1$  surfaces are shown in Figs. 1, and 2. The largest and the smallest values in the figures represent  $\pm 1\sigma$  errors of corresponding parameters.

$ \delta C_i $	Cases				
	b	c	d	e	f
$ \delta C_1 $	0.27	0.27	0.04	0.07	0.07
$ \delta Re(C_S) $	0.40	-	-	0.05	-
$ \delta Re(C_T) $	-	0.30	-	-	0.04
$ \delta(Im(C_S)Im(C_T)) $	0.11	0.11	0.01	-	-

TABLE IX: Numerical values of  $|\delta C_i|$  extracted from the  $\tau$  forward-backward asymmetry in  $B \rightarrow D\tau\nu_\tau$ .

### A. Discussions

For case  $a$ , the uncertainties obtained from the simultaneous extraction of all the Wilson coefficients from the observable  $R(D)$  shows that <sup>4</sup>

$$\frac{|\delta C_4|}{|\delta C_5|} \approx \frac{|\delta Re(C_S)|}{|\delta Re(C_T)|} \sim 1, \quad \frac{\delta |C_S|^2}{\delta |C_T|^2} \sim 2, \quad (14)$$

which shows that  $R(D)$  is equally sensitive to the real part of  $C_S$  and  $C_T$ . The above result does not allow a direct comparison between the sensitivities to the imaginary part of the coefficients. The results obtained for all the other cases are shown in Tab. VII, and in Figs.1a, 1b and 1c. We note that if the Wilson coefficients are purely imaginary then  $R(D)$  is more sensitive to  $Im(C_S)$  compared to  $Im(C_T)$ . Also, it is important to note that this observable is more sensitive to the real part of the coefficients than the imaginary part. Comparing all the different cases considered for  $R(D)$ , it would be difficult to comment on the overall sensitivity of this observable to a particular type of NP interaction. However, in the next section we will see that there are distinct regions of  $q^2$  which are sensitive to either scalar or tensor type interactions.

On the other hand, the analysis of  $P_\tau^R(q^2)$  for case  $a$  gives

$$\frac{|\delta C_4|}{|\delta C_5|} \approx \frac{|\delta Re(C_S)|}{|\delta Re(C_T)|} \sim 0.5, \quad \frac{\delta |C_S|^2}{\delta |C_T|^2} \sim 2, \quad (15)$$

<sup>4</sup> The results corresponding to the case  $a$  are not shown in the table, because the extracted uncertainties are very large ( $\gg 1$ ).

which shows an improvement in sensitivity to  $Re(C_S)$  compared to  $Re(C_T)$ . The results obtained from all the other relevant cases are shown in Table VII, and in Figs. 1d, 1e, and 1f, which allow a case by case comparison between the results obtained from  $R(D)$  and  $P_\tau^R$ . Interestingly, the extracted uncertainties are less compared to that extracted in  $R(D)$ . The sensitivity of this observable to tensor interaction is a little less, compared to scalar interaction, but it can be extracted with uncertainties less than 1.

As shown in Table VIII, and in Fig. 2, the observables like  $R(D^*)$  and  $P_\tau^{R*}$  are more sensitive to  $|C_T|^2$  compared to any other new Wilson coefficients, almost in all the cases  $|C_T|^2$  and  $Re(C_T)$  can be extracted with small uncertainties. A case by case comparison shows that the above observables are more sensitive to  $C_T$  than  $C_S$ , and  $\delta Re(C_T) < \delta Re(C_{V_2})$  but they are of same order. Also, when  $C_T$  is purely imaginary, we find  $\delta Im(C_T) \approx \delta Re(C_{V_2})$ , though  $P_\tau^{R*}$  have little better sensitivity to  $Im(C_T)$ . Therefore, these observables alone won't allow us to distinguish the contributions from right handed vector current to that of a tensor current. However, in the next section we will see that a bin by bin analysis of the  $q^2$  distribution of the differential decay rate allows to discriminate the effects of these interactions.

However, when  $C_T = 0$ , both the observables are almost equally sensitive, though  $\delta Re(C_S) < \delta Re(C_{V_2})$ , to the real part of the vector and scalar Wilson coefficients. In case  $C_S$  is purely imaginary,  $\delta Re(C_{V_2}) \ll \delta Im(C_S)$  i.e the observables are less sensitive to the imaginary part of  $C_S$  compared to the real parts of  $C_{V_2}$  and  $C_S$ . Again, we note that the extracted errors on  $C_i$ s from  $P_\tau^{R*}$  are smaller than those in  $R(D^*)$ .

$ \delta C_i $	Cases					
	2*	3*	4*	5*	6*	7*
$ \delta C_1 $	1.30	2.41	0.40	0.27	0.52	0.04
$\delta C_T ^2$	0.12	0.08	0.04	0.04	0.03	-
$ \delta Re(C_S) $	16.30	-	1.72	-	-	0.02
$ \delta Re(C_T) $	-	1.06	-	0.12	-	-
$ \delta(Im(C_S)Im(C_T^*)) $	2.48	2.41	-	-	0.26	-

TABLE X: Numerical values of  $|\delta C_i|$  extracted from  $\tau$  forward backward asymmetry in  $B \rightarrow D^* \tau \nu_\tau$ .

The results of the analysis of forward-backward asymmetries and  $D^*$  polarisation are given in Tables IX, X, and XI respectively. The forward-backward asymmetry in  $B \rightarrow D \tau \nu_\tau$  is equally sensitive to the scalar and tensor type interactions.

For case 1\* in  $A_{FB}^{R*}$ , we find

$$\frac{\delta C_1}{\delta|C_T|^2} \approx 1, \quad \frac{\delta C_2}{\delta|C_T|^2} \approx 24, \quad (16)$$

and

$$\frac{\delta C_2}{\delta Re(C_T)} \approx 12, \quad (17)$$

where  $C_1$  and  $C_2$  are the functions of the Wilson coefficients of the vector operators. The approximate forms are given by

$$C_1 \approx 1 + 2Re(C_{V_1}), \quad C_2 \approx 1 + 2Re(C_{V_1}) - 2Re(C_{V_2}). \quad (18)$$

It indicates that the  $\tau$  forward-backward asymmetry in  $B \rightarrow D^* \tau \nu_\tau$  is more sensitive to tensor Wilson coefficients than to a vector, in particular to  $C_{V_2}$ . In order to understand it better, we define

$$C_{12} = C_1 - C_2 \approx 2Re(C_{V_2}). \quad (19)$$

Therefore, a simple calculation shows that

$$\frac{\delta Re(C_{V_2})}{\delta Re(C_T)} = \frac{1}{2} \frac{\delta C_{12}}{\delta Re(C_T)} \approx 6. \quad (20)$$

In all the other cases with  $C_{V_2} = 0$ , the  $A_{FB}$  in  $B \rightarrow D^* \tau \nu_\tau$  is more sensitive to the tensor interaction compared to the scalar. On the other hand the  $D^*$  polarisation is equally sensitive to the scalar and tensor interactions. Therefore, if future data shows large deviations from the SM predictions in all the observables like  $R(D^*)$ ,  $A_{FB}^*$ , and  $D^*$  polarisation, that can be thought of as an indication of the presence of a new tensor type interaction. On other hand, if a deviation is only in  $R(D^*)$  and not in the others, that could be an indication of a new vector interaction.

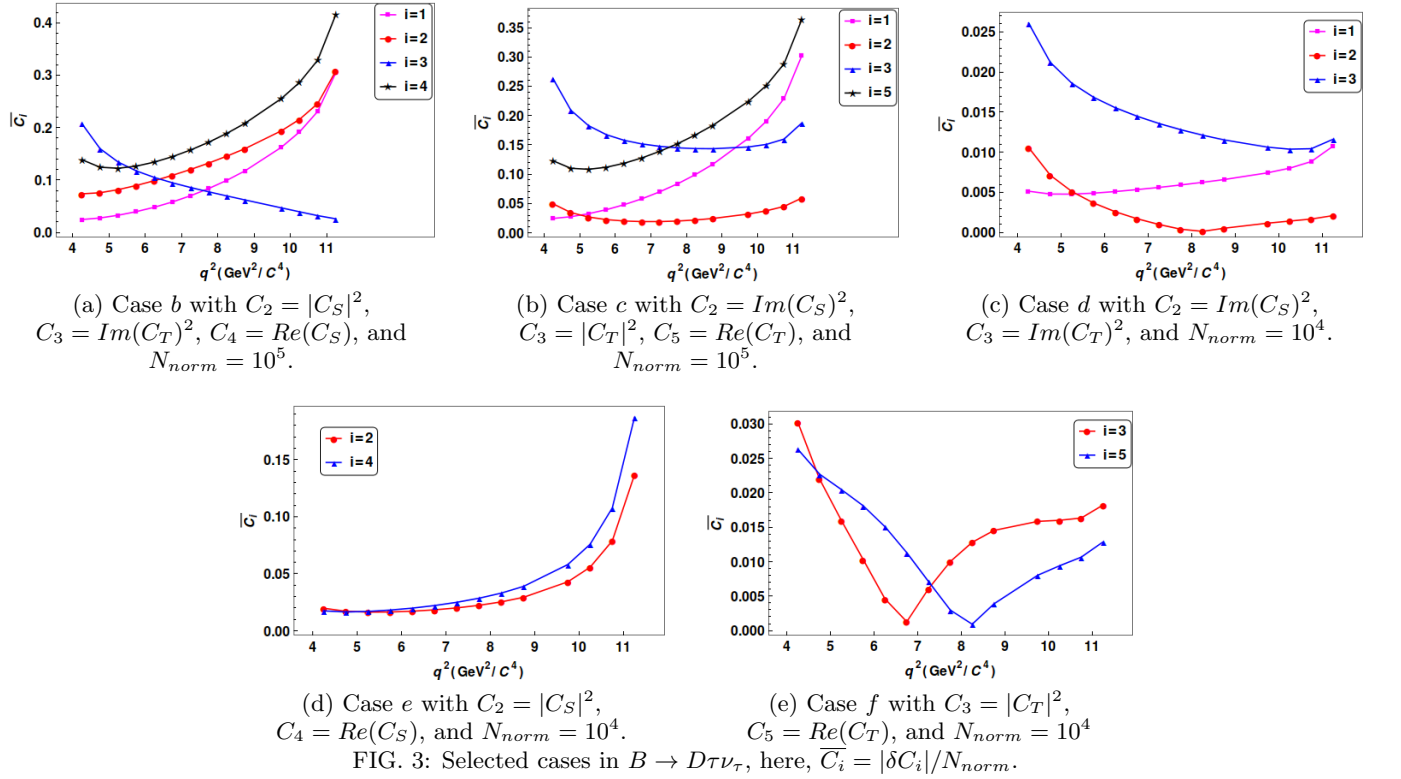


Cases	A	B	C	D	E	F	G	H
$ \delta C_i $								
$ \delta C_1 $	3.58	0.74	1.41	0.12	0.05	1.41	0.05	0.1
$\delta C_S ^2$	16.63	3.39	0.55	0.55	0.77	-	0.54	-
$\delta C_T ^2$	2.53	0.09	0.41	0.01	-	0.41	-	0.01
$ \delta Re(C_S) $	7.05	1.40	-	-	0.20	-	-	-
$ \delta Re(C_T) $	5.07	-	1.00	-	-	1.00	-	-

TABLE XI: The results obtained from the analysis of the  $D^*$  polarisation asymmetry in the decay  $B \rightarrow D^* \tau \nu_\tau$ .

### B. Bin-by-bin analysis

In general, the sensitivity to various NP interactions may also be  $q^2$  dependent. Hence, we analyse the bin-by-bin  $q^2$  distribution of the differential decay rate of  $B \rightarrow D^{(*)} \tau \nu_\tau$  to look for more possibilities, and zoom in to the regions of  $q^2$ , within which the sensitivity to a specific type of new interaction is much larger than most other regions. In general the  $\delta C_i$ s extracted from individual bins are very large, therefore in the figs. 3, 4 we plot  $\bar{\delta C}_i = \delta C_i / N_{norm}$ , where  $N_{norm}$  is some number used to normalised  $\delta C_i$ .



The results obtained from the analysis of the  $q^2$  distribution of differential decay rate in  $B \rightarrow D \tau \nu_\tau$  are presented in fig. 3, where the variations of the  $\delta C_i$ s with  $q^2$  are shown. The normalised uncertainties in the simultaneous extraction of  $|C_S|^2$ ,  $|C_T|^2$ ,  $Re(C_T)$  and  $Re(C_S)$ , and their variations with  $q^2$  are shown in figs. 3a and 3b respectively. On the other hand the variations of  $\delta|C_S|^2$ , and  $\delta Re(C_S)$  with  $q^2$  when  $C_T = 0$  are shown in fig. 3d, while that for  $\delta|C_T|^2$ , and  $\delta Re(C_T)$  when  $C_S = 0$  are shown in fig. 3e. We note that in the low  $q^2$  region ( $\lesssim 7 GeV^2/c^4$ ) the differential decay rate is sensitive to the scalar interaction<sup>5</sup>, the sensitivity to tensor interaction in this region is very weak, whereas in the high  $q^2$  region ( $\gtrsim 7 GeV^2/c^4$ ) it is rather sensitive to the tensor interaction. In case the Wilson coefficients are purely imaginary, in all the  $q^2$  regions, the decay rate distribution is sensitive more to the scalar interaction (fig. 3c) than the others.

As we noted earlier,  $R(D^*)$  is equally sensitive to  $C_{V_2}$  and  $C_T$  (case  $a^*$ ), however, the analysis of the differential decay rate distributions show that (figs. 4e and 4d) it is sensitive to tensor interaction only in the very high and low

<sup>5</sup> In very low  $q^2$  regions the  $q^2$  distribution is also sensitive to  $C_1$ .

$q^2$  regions, and it is sensitive to  $C_{V_2}$  in all the  $q^2$  regions except the very low  $q^2$  region. In fig. 4a the variations of  $\delta Re(C_{V_2})$ ,  $\delta Re(C_S)$ , and  $\delta |C_S|^2$  with the  $q^2$  in the case  $C_T = 0$  are shown, we note that in all the  $q^2$  regions the decay rate is equally sensitive to vector and scalar interactions except in the very low  $q^2$  region, where the sensitivity to  $Re(C_S)$  is better than that to  $Re(C_{V_2})$ . We also study the cases when the NP interaction is scalar type. The  $q^2$  distribution of the extracted errors on the respective parameters is shown in fig. 4c, which indicates that the decay rate is sensitive to scalar interactions only in the low  $q^2$  region. If  $C_S$  and  $C_T$  are purely imaginary than the  $q^2$  distribution of the decay rate is sensitive to the tensor interactions in all the  $q^2$  regions (fig. 4b).

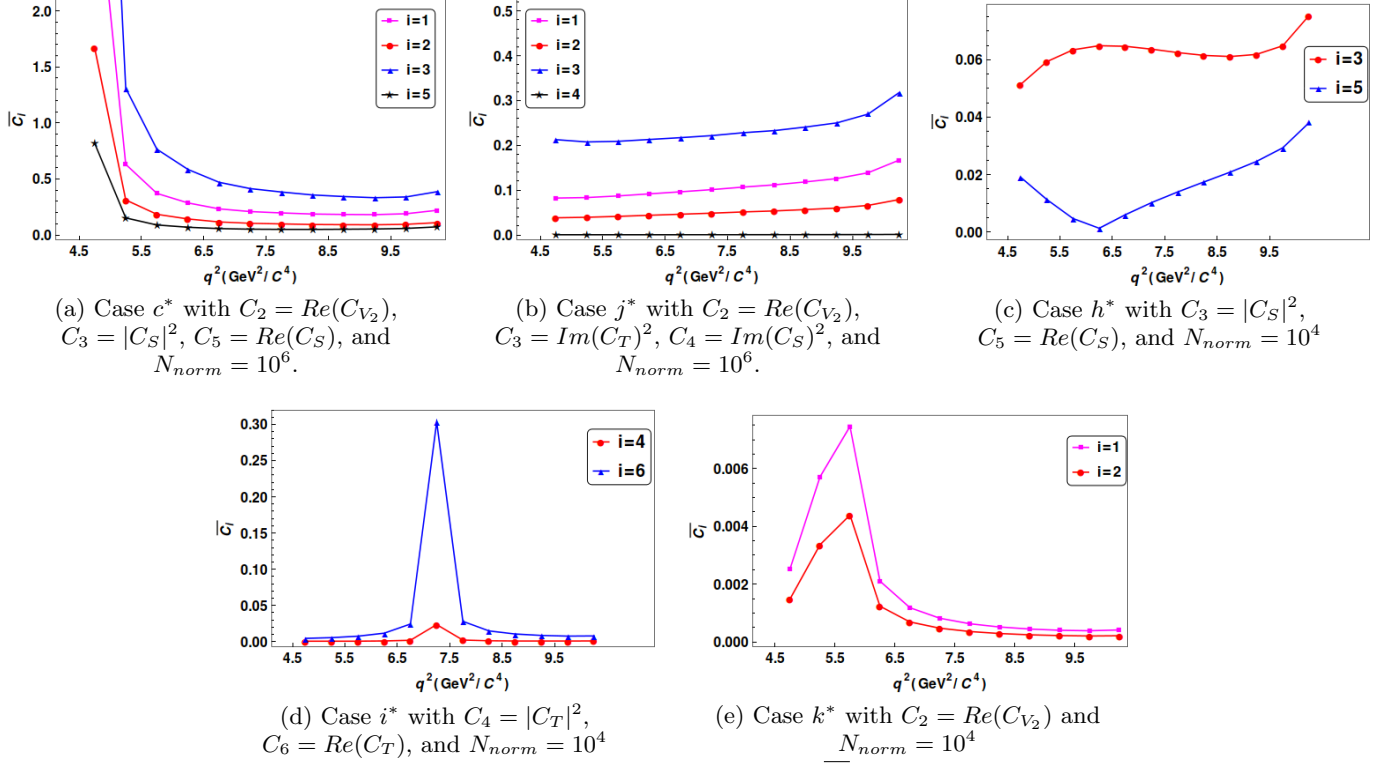


FIG. 4: Selected cases in  $B \rightarrow D^* \tau \nu_\tau$ , here,  $\overline{C}_i = |\delta C_i|/N_{norm}$ .

All these studies suggest that we could gain in NP sensitivity if we focus on specific  $q^2$  regions, which we may lose in the full  $q^2$ -integrated observables. We note that the sensitivity to a particular type of interaction is limited to particular regions of  $q^2$ . Therefore, the experimental data in the specific regions of  $q^2$  could help us a better interpretation of the type of NP interactions, which may not be obtainable from  $q^2$  integrated observables. As for example, if we see large deviations in data only in the very high and very low  $q^2$  regions, that can be interpreted as due to the presence of a tensor interaction (fig. 4d). On the other hand, if we see deviations only in the low  $q^2$  ( $< 7$ ) bins, that could be due to a new scalar interaction (fig. 4c). Finally, if data shows deviations in most of the  $q^2$  bin except the very low  $q^2$ , this can be due to the presence of new vector interaction (fig. 4e).

In order to explain our point we take the example of the  $q^2$  distributions of the measured events in  $B \rightarrow D^{(*)} \tau \nu_\tau$ , which are shown in Fig.(5). The plots are generated using the data given in ref. [2, 23, 24]. The predicted  $q^2$  distributions in SM with the central values of the form factors are shown by black lines, blue dotted lines represent the errors in SM. In Fig.(5a), we see that the data is not fully consistent with the SM in the region  $8.0 < q^2 < 11$ , which is the region where the decay rate distribution is sensitive to tensor interaction, as analysed above in the decay  $B \rightarrow D \tau \nu_\tau$ . At the moment it is hard to conclude anything, and we have to wait for better statistics. From Fig.(5b) we see distinct regions of  $q^2$  where the data is not fully consistent with the SM prediction, and our analysis suggests that those regions could potentially be very sensitive to NP effects. Again, because of poor statistics it is premature to conclude anything. Therefore, the experimental effort should be in gathering more statistics in specific regions of  $q^2$  potentially sensitive to NP, which may in turn help the clean extraction of NP couplings.

As mentioned above, the numerical estimates are done with central values of all the relevant parameters taken from [22]. Numerical instability of our results could be main source of uncertainty in our estimates. The numerical results of  $X_{ij}$ , which depend on the matrix inversion of  $M_{ij}$ , are often unstable; even a tiny variation of  $M_{ij}$  could change  $X_{ij}$  significantly. This is why, when we estimate the statistical uncertainties in simultaneous extractions of the Wilson coefficients, we allowed only stable solutions. We calculate the selected  $\delta C_i$  first to  $m^{th}$  and then to

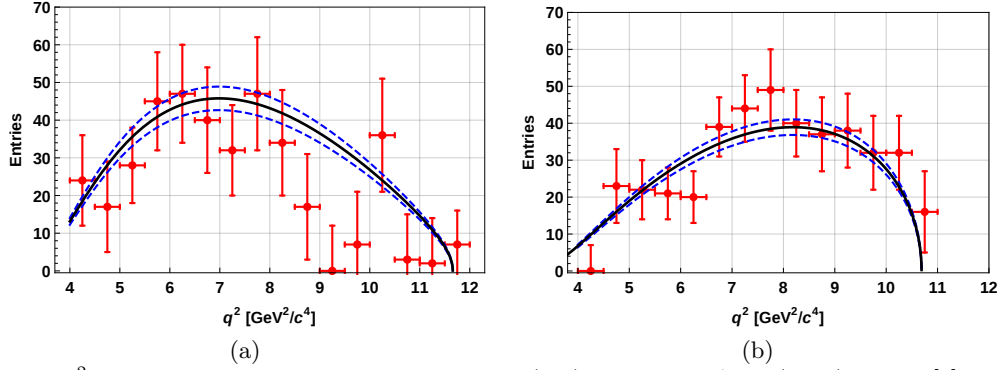


FIG. 5: Measured  $q^2$  distribution of the events in  $B \rightarrow D\tau\nu_\tau$  (left) and  $B \rightarrow D^*\tau\nu_\tau$  (right) decays [2]. The black lines represent the  $q^2$  distribution predicted in the SM, obtained from the respective differential branching fractions.  $(m-1)^{th}$  decimal places, and obtain  $\delta C_i^{[m]}$  and  $\delta C_i^{[(m-1)]}$  respectively. We consider the results as stable only when  $(\delta C_i^{[m]} - \delta C_i^{[(m-1)]})/\delta C_i^{[m]} < 0.01$ . We checked the stability up to  $m = 10$ , and in most of the cases presented above, our results are very much stable, and the error due to this is negligible. As we can see from the expressions of  $\delta C_i$ , the other sources of errors in our estimates are given by the errors in  $f_i(q^2)$ ,  $\sigma_P$ ,  $\mathcal{L}_{eff}$ , and  $\mathcal{B}_\ell$ . It is straight forward to estimate the errors due to  $\sigma_P$ ,  $\mathcal{L}_{eff}$ , and  $\mathcal{B}_\ell$ .

Cases		$\delta C_i$	$\delta C_i^+$	$\delta C_i^-$	$\pm\%Err.$
d	$C_1$	0.082	0.079	0.087	5.032
	$Im(C_S)^2$	0.013	0.013	0.014	5.032
	$Im(C_T)^2$	0.168	0.160	0.177	5.032
e	$C_1$	0.240	0.229	0.253	5.031
	$ C_S ^2$	0.274	0.261	0.289	5.031
	$Re(C_S)$	0.354	0.337	0.373	5.031

TABLE XII: Numerical values of  $\delta C_i$ s, and  $\delta C_i^+$  ( $\delta C_i^-$ ) considering +10% (-10%) errors in  $f_i(q^2)$  for few cases of  $R(D)$ . The % error is given by  $(\delta C_i - \delta C_i^\pm)/\delta C_i$ .

However, the estimate due to  $f_i(q^2)$ s are not that straight forward since  $M_{ij}$ s depend solely upon them. The main sources of uncertainties in  $f_i$ s, including the SM, are the form-factors. Errors due to other parameters, like CKM element etc, are canceled in the ratios. In the tables XII, and XIII, we consider a few cases and give a rough estimate of the uncertainties due to the errors in  $f_i(q^2)$ . The overall error is about  $\pm 5\%$  in the extraction of  $\delta C_i$ s, if we consider the errors in  $f_i(q^2)$ s are about  $\pm 10\%$ . We also estimate the errors in  $\delta C_i$  by considering the actual errors in all the form-factors given in ref. [22], and find that they are even smaller than whatever we have shown in the above mentioned tables. Finally, we would like to comment that the estimated errors due to form-factors, and the other experimental parameters will have almost equal impact on all the extracted  $\delta C_i$ s, which is also small. Therefore, our conclusions about the relative sensitivities will not change.

Cases		$\delta C_i$	$\delta C_i^+$	$\delta C_i^-$	$\pm\%Err.$
$f^*$	$C_1$	0.448	0.427	0.472	5.032
	$Re(C_{V_2})$	0.211	0.201	0.222	5.032
	$Im(C_T)^2$	0.006	0.0058	0.0065	5.032
$g^*$	$C_1$	0.042	0.040	0.044	5.032
	$Im(C_S)^2$	0.961	0.916	1.013	5.032
	$Im(C_T)^2$	0.0048	0.0046	0.0051	5.032

TABLE XIII: Numerical values of  $\delta C_i$ s, and  $\delta C_i^+$  ( $\delta C_i^-$ ) considering +10% (-10%) errors in  $f_i(q^2)$  for few cases of  $R(D^*)$ . The % error is given by  $(\delta C_i - \delta C_i^\pm)/\delta C_i$ .

#### IV. SUMMARY

We use the optimal observable technique to test the sensitivities of the various observables in  $B \rightarrow D^{(*)}\tau\nu_\tau$  to the various NP interactions, like new vector, scalar and tensor interactions. Numerically, we find that the observables in  $B \rightarrow D\tau\nu_\tau$  are more or less equally sensitive to scalar and tensor interactions, only exception is the  $\tau$  polarisation

asymmetry, where  $\delta Re(C_S) < \delta Re(C_T)$  but they are of same order. Therefore, even if the measured values of the observables deviate from their SM expectations, a priori it would be hard to decide what type of new interaction will it be. However, the analysis of the  $q^2$  distribution of the decay rate allows us to separate the regions of  $q^2$  which are sensitive to scalar interaction (low  $q^2$ ) and tensor interaction (high  $q^2$ ).

The overall sensitivity of the observables in  $B \rightarrow D^* \tau \nu_\tau$  is more towards tensor interactions, in particular to  $|C_T|^2$ . Also, we note that  $\delta Re(C_T) < \delta Re(C_{V_2})$  but they are of same order, hence, we need better statistics to distinguish their effects. The decay  $B \rightarrow D^* \tau \nu_\tau$  has very poor sensitivity to scalar interaction compared to the tensor interaction, the only exceptions being the  $D^*$  polarisation,  $A_{FB}^{R*}$ . However, in the absence of tensor interactions, the decay  $B \rightarrow D^* \tau \nu_\tau$  is equally sensitive to real part of both the vector and scalar Wilson coefficients, sensitivity to  $|C_S|^2$  is much less compared to the real parts. However, the analysis of the  $q^2$  distributions of the decay rate shows distinct regions of  $q^2$ , which are sensitive to vector, scalar, and tensor interactions respectively. These sensitivities are lost in the full  $q^2$  integrated observables. Present data on different bins do not have sufficient statistics to conclude anything, more precise data could help us to pinpoint the type of NP interaction. Therefore, in an experiment, the priority should be given to gaining statistics at those regions of  $q^2$ .

We note that both the decay modes are more sensitive to the real part of the coefficients compared to imaginary part. Among the various observables,  $\tau$  polarisation asymmetries have better sensitivity to the relevant new coefficients ( $C_i$ ); the uncertainties on the extracted  $C_i$ s are either less or comparable to that obtained in others. Therefore, future data on  $\tau$  polarisation asymmetries could put tighter constraints on the NP parameter space.

## V. ACKNOWLEDGEMENT

We would like to thank Subhaditya Bhattacharya for useful discussions on optimal-observable analysis. SN would also like to thank Thomas Kuhr and Bipul Bhuyan for useful discussions.

## VI. APPENDIX

In the following tables, the various  $f_i(q^2)$  for different observables used in our analysis are shown.

$f_i$ \backslash Obs	$R(D)$	$P_\tau^R$
$f_1$	$\mathcal{G} \left( \left( 1 + \frac{m_\tau^2}{2q^2} \right) H_{V,0}^s{}^2 + \frac{3}{2} \frac{m_\tau^2}{q^2} H_{V,t}^s{}^2 \right)$	$\mathcal{G} \left( \left( -1 + \frac{m_\tau^2}{2q^2} \right) H_{V,0}^s{}^2 + \frac{3}{2} \frac{m_\tau^2}{q^2} H_{V,t}^s{}^2 \right)$
$f_2$	$\frac{3}{2} \mathcal{G} H_S^s{}^2$	$\frac{3}{2} \mathcal{G} H_S^s{}^2$
$f_3$	$8\mathcal{G} \left( 1 + \frac{2m_\tau^2}{q^2} \right) H_T^s{}^2$	$8\mathcal{G} \left( 1 - \frac{2m_\tau^2}{q^2} \right) H_T^s{}^2$
$f_4$	$3\mathcal{G} \frac{m_\tau}{\sqrt{q^2}} H_S^s H_{V,t}^s$	$3\mathcal{G} \frac{m_\tau}{\sqrt{q^2}} H_S^s H_{V,t}^s$
$f_5$	$-12\mathcal{G} \frac{m_\tau}{\sqrt{q^2}} H_T^s H_{V,0}^s$	$4\mathcal{G} \frac{m_\tau}{\sqrt{q^2}} H_T^s H_{V,0}^s$

TABLE XIV:  $f_i$ s for  $R_D$  and  $\tau$  polarisation asymmetry in  $B \rightarrow D\tau\nu_\tau$ .

$f_i$ \backslash Obs	$R(D^*)$	$P_\tau^{R*}$
$f_1$	$\mathcal{G}^* \left( \left( 1 + \frac{m_\tau^2}{2q^2} \right) (H_{V,+}^2 + H_{V,-}^2 + H_{V,0}^2) + \frac{3}{2} \frac{m_\tau^2}{q^2} H_{V,t}^2 \right)$	$\mathcal{G}^* \left( \left( -1 + \frac{m_\tau^2}{2q^2} \right) (H_{V,+}^2 + H_{V,-}^2 + H_{V,0}^2) + \frac{3}{2} \frac{m_\tau^2}{q^2} H_{V,t}^2 \right)$
$f_2$	$-2\mathcal{G}^* \left( \left( 1 + \frac{m_\tau^2}{2q^2} \right) (H_{V,0}^2 + 2H_{V,+}H_{V,-}) + \frac{3}{2} \frac{m_\tau^2}{q^2} H_{V,t}^2 \right)$	$\mathcal{G}^* \left( \left( 2 - \frac{m_\tau^2}{q^2} \right) (H_{V,0}^2 + 2H_{V,+}H_{V,-}) - 3 \frac{m_\tau^2}{q^2} H_{V,t}^2 \right)$
$f_3$	$\frac{3}{2} \mathcal{G}^* H_S^2$	$\frac{3}{2} \mathcal{G}^* H_S^2$
$f_4$	$8\mathcal{G}^* \left( \left( 1 + \frac{2m_\tau^2}{q^2} \right) (H_{T,+}^2 + H_{T,-}^2 + H_{T,0}^2) \right)$	$8\mathcal{G}^* \left( \left( 1 - \frac{2m_\tau^2}{q^2} \right) (H_{T,+}^2 + H_{T,-}^2 + H_{T,0}^2) \right)$
$f_5$	$3\mathcal{G}^* \frac{m_\tau}{\sqrt{q^2}} H_S H_{V,t}$	$3\mathcal{G}^* \frac{m_\tau}{\sqrt{q^2}} H_S H_{V,t}$
$f_6$	$-12\mathcal{G}^* \frac{m_\tau}{\sqrt{q^2}} (H_{T,0}H_{V,0} + H_{T,+}H_{V,+} - H_{T,-}H_{V,-})$	$4\mathcal{G}^* \frac{m_\tau}{\sqrt{q^2}} (H_{T,0}H_{V,0} + H_{T,+}H_{V,+} - H_{T,-}H_{V,-})$
$f_7$	$12\mathcal{G}^* \frac{m_\tau}{\sqrt{q^2}} (H_{T,0}H_{V,0} + H_{T,+}H_{V,-} - H_{T,-}H_{V,+})$	$-4\mathcal{G}^* \frac{m_\tau}{\sqrt{q^2}} (H_{T,0}H_{V,0} + H_{T,+}H_{V,-} - H_{T,-}H_{V,+})$

TABLE XV:  $f_i$ s for  $R_{D^*}$  and  $\tau$  polarisation asymmetry in  $B \rightarrow D^* \tau \nu_\tau$ .

$f_i$ \ Obs	$\mathcal{A}_{\mathcal{F}B}^{\mathcal{R}}$	$\mathcal{A}_{\mathcal{F}B}^{\mathcal{R}*}$	$P_{D^*}^R$
$f_1$	$\mathcal{F} \left( \frac{m_\tau^2}{q^2} H_{V,0}^s H_{V,t}^s \right)$	$\frac{1}{2} \mathcal{F}^* (H_{V,+}^2 - H_{V,-}^2)$	$\mathcal{G}^* \left( \left( 1 + \frac{m_\tau^2}{2q^2} \right) H_{V,0}^2 + \frac{3}{2} \frac{m_\tau^2}{q^2} H_{V,t}^2 \right)$
$f_2$	$\mathcal{F} \left( \frac{m_\tau}{\sqrt{q^2}} H_{V,0}^s H_S^s \right)$	$\mathcal{F}^* \frac{m_\tau^2}{q^2} H_{V,0} H_{V,t}$	$\frac{3}{2} \mathcal{G}^* H_S^2$
$f_3$	$-4\mathcal{F} \left( \frac{m_\tau}{\sqrt{q^2}} H_{V,t}^s H_T^s \right)$	$8\mathcal{F}^* \frac{m_\tau^2}{q^2} (H_{T,+}^2 - H_{T,-}^2)$	$8\mathcal{G}^* \left( 1 + \frac{2m_\tau^2}{q^2} \right) H_{T,0}^2$
$f_4$	$-4\mathcal{F} H_S^s H_T^s$	$\mathcal{F}^* \frac{m_\tau}{\sqrt{q^2}} H_S H_{V,0}$	$3\mathcal{G}^* \frac{m_\tau}{\sqrt{q^2}} H_S H_{V,t}$
$f_5$	–	$-4\mathcal{F}^* \frac{m_\tau}{\sqrt{q^2}} (H_{T,0} H_{V,t} + H_{T,+} H_{V,+} + H_{T,-} H_{V,-})$	$-12\mathcal{G}^* \frac{m_\tau}{\sqrt{q^2}} H_{T,0} H_{V,0}$
$f_6$	–	$4\mathcal{F}^* \frac{m_\tau}{\sqrt{q^2}} (H_{T,0} H_{V,t} + H_{T,+} H_{V,-} + H_{T,-} H_{V,+})$	–
$f_7$	–	$-4\mathcal{F}^* H_{T,0} H_S$	–

TABLE XVI:  $f_i$ s for  $\tau$  forward-backward asymmetries in  $B \rightarrow D^{(*)} \tau \nu_\tau$  decays, and  $D^*$  polarisation asymmetry in  $B \rightarrow D^* \tau \nu_\tau$ .

The expressions for  $\mathcal{F}$ ,  $\mathcal{F}^*$ ,  $\mathcal{G}$ ,  $\mathcal{G}^*$  are given by [5]

$$\begin{aligned}
\mathcal{G} &= \frac{\tau_B}{\mathcal{B}(B \rightarrow D l \nu)} \frac{G_F^2 |V_{cb}|^2}{192\pi^3 m_B^3} q^2 \sqrt{\lambda_D(q^2)} \left( 1 - \frac{m_\tau^2}{q^2} \right)^2, \\
\mathcal{G}^* &= \frac{\tau_B}{\mathcal{B}(B \rightarrow D^* l \nu)} \frac{G_F^2 |V_{cb}|^2}{192\pi^3 m_B^3} q^2 \sqrt{\lambda_{D^*}(q^2)} \left( 1 - \frac{m_\tau^2}{q^2} \right)^2 \\
\mathcal{F} &= \frac{\tau_B}{\mathcal{B}(B \rightarrow D l \nu)} \frac{G_F^2 |V_{cb}|^2}{128\pi^3 m_B^3} q^2 \sqrt{\lambda_D(q^2)} \left( 1 - \frac{m_\tau^2}{q^2} \right)^2 \\
\mathcal{F}^* &= \frac{\tau_B}{\mathcal{B}(B \rightarrow D^* l \nu)} \frac{G_F^2 |V_{cb}|^2}{128\pi^3 m_B^3} q^2 \sqrt{\lambda_{D^*}(q^2)} \left( 1 - \frac{m_\tau^2}{q^2} \right)^2
\end{aligned} \tag{21}$$

- 
- [1] I. Adachi *et al.* [Belle Collaboration], arXiv:0910.4301 [hep-ex].
- [2] J. P. Lees *et al.* [BaBar Collaboration], Phys. Rev. D **88**, no. 7, 072012 (2013) [arXiv:1303.0571 [hep-ex]].
- [3] S. Fajfer, J. F. Kamenik and I. Nisandzic, Phys. Rev. D **85**, 094025 (2012) [arXiv:1203.2654 [hep-ph]].
- [4] M. Tanaka, Z. Phys. C **67**, 321 (1995) [hep-ph/9411405].
- [5] Y. Sakaki, M. Tanaka, A. Tayduganov and R. Watanabe, Phys. Rev. D **88**, no. 9, 094012 (2013) [arXiv:1309.0301 [hep-ph]].
- [6] M. Duraisamy, P. Sharma and A. Datta, Phys. Rev. D **90**, no. 7, 074013 (2014) [arXiv:1405.3719 [hep-ph]].
- [7] M. Tanaka and R. Watanabe, Phys. Rev. D **87**, no. 3, 034028 (2013) [arXiv:1212.1878 [hep-ph]].
- [8] Y. Sakaki, M. Tanaka, A. Tayduganov and R. Watanabe, Phys. Rev. D **91**, no. 11, 114028 (2015) [arXiv:1412.3761 [hep-ph]].
- [9] M. Freytsis, Z. Ligeti and J. T. Ruderman, Phys. Rev. D **92**, no. 5, 054018 (2015) [arXiv:1506.08896 [hep-ph]].
- [10] S. Fajfer, J. F. Kamenik and I. Nisandzic, Phys. Rev. D **85**, 094025 (2012) [arXiv:1203.2654 [hep-ph]].
- [11] P. Biancofiore, P. Colangelo and F. De Fazio, Phys. Rev. D **87**, no. 7, 074010 (2013) [arXiv:1302.1042 [hep-ph]].
- [12] R. Aaij *et al.* [LHCb Collaboration], Phys. Rev. Lett. **115**, no. 11, 111803 (2015) [arXiv:1506.08614 [hep-ex]].
- [13] M. Huschle *et al.* [Belle Collaboration], arXiv:1507.03233 [hep-ex].
- [14] M. Davier, L. Duflot, F. Le Diberder and A. Rouge, Phys. Lett. B **306**, 411 (1993).
- [15] M. Diehl and O. Nachtmann, Z. Phys. C **62**, 397 (1994).
- [16] D. Atwood and A. Soni, Phys. Rev. D **45**, 2405 (1992).
- [17] J. F. Gunion, B. Grzadkowski and X. G. He, Phys. Rev. Lett. **77**, 5172 (1996) [hep-ph/9605326].
- [18] M. Diehl and O. Nachtmann, Eur. Phys. J. C **1**, 177 (1998) [hep-ph/9702208].
- [19] B. Grzadkowski, Z. Hioki, K. Ohkuma and J. Wudka, Phys. Lett. B **593**, 189 (2004) [hep-ph/0403174].
- [20] S. Davidson, D. C. Bailey and B. A. Campbell, Z. Phys. C **61**, 613 (1994) [hep-ph/9309310].
- [21] E. Ponton, arXiv:1207.3827 [hep-ph].
- [22] M. Okamoto *et al.*, Nucl. Phys. Proc. Suppl. **140**, 461 (2005) [hep-lat/0409116]; J. A. Bailey *et al.* [Fermilab Lattice and MILC Collaborations], PoS LATTICE **2010**, 311 (2010) [arXiv:1011.2166 [hep-lat]]; Y. Amhis *et al.* [Heavy Flavor Averaging Group Collaboration], arXiv:1207.1158 [hep-ex].
- [23] B. Aubert *et al.* [BaBar Collaboration], Phys. Rev. Lett. **104**, 011802 (2010) [arXiv:0904.4063 [hep-ex]].
- [24] B. Aubert *et al.* [BaBar Collaboration], Phys. Rev. Lett. **100**, 151802 (2008) [arXiv:0712.3503 [hep-ex]].